Supplementary Information

Enhancing Efficiency and Stability of Perovskite Solar Cells Using ALD-Al_2O_3 as an Electron Transport Layer Buffer

Zhengyi Sun*, Huiru Li, Yuan Li, Chaojun Sun

State Key Laboratory of Flexible Electronics, School of Flexible Electronics (Future Technologies), Nanjing Tech University, 30 South Puzhu Road, Nanjing 211816, China

*Corresponding author: iamzysun@njtech.edu.cn

1. Experimental section

Materials: Lead iodide (PbI_2), methylammonium iodide (MAI, CH_3NH_3I), Spiro-OMe TAD, LiTFSI, 4-tert-butylpyridine (t-BP), and Fullerene (C_{60}) were purchased from Xi'an Yuri Solar Co., Ltd. Bathocuproine (BCP). Carbon paste were purchased from Shanghai Materwin New Materials Co, Ltd. Trimethylaluminum (TMA) was purchased from Nanjing ai mou yuan Scientific equipment Co., Ltd. Nickel nitrate hexahydrate ($Ni(NO_3)_2 \cdot 6H_2O$), ethylenediamine, ethylene glycol and acetonitrile were purchased from Aladdin. N,N-Dimethylformamide (DMF) was purchased from Damas-beta. Dimethyl sulfoxide (DMSO) was purchased from Sigma-Aldrich. $SnO_2 \cdot 15\%H_2O$ and chlorobenzene (CB) were purchased from Alfa Aesar. Ag and Au were purchased from Zhong Nuo Advanced Material (Shanghai) Technology Co., Ltd.

Device fabrication:

The ITO glass was cleaned with detergent and ultra-pure water, and the ITO glass was ultrasonic treated with ultra-pure water, acetone and isopropyl alcohol successively for 20 minutes. Then it was dried in a vacuum oven, and finally treated with UV-Ozone cleaner for 20 minutes to enhance the surface wettability of ITO glass.

(1) n-i-p device：

ALD Al_2O_3 film: Compact Al_2O_3 layers were deposited by an atomic layer deposition system (MNT Micro 100), using the precursors TMA and H_2O, and the precursors were heated to 120°C to obtain sufficient reaction vapor pressure. The deposition temperature in the reaction chamber is maintained at 75°C. Process pressure is 2.5 Torr, and high purity N_2 (flow rate, 10sccm) as carrier and purge gas. When the purge, pump line and heater reach the set temperature, the equipment begins to operate as designed. The ALD procedure is as follows: 10 ms TMA pulse (0.15 Torr), 35 s N_2 purge, 10 ms H_2O pulse (0.15 Torr) and 25 s N_2 purge for each complete cycle. ALD Al_2O_3 growth is observed at a deposition rate of about 0.1 nm/cycle, and Al_2O_3 layers of about 2 nm can be obtained with 20 cycles.

SnO_2 Film: $SnO_2 \cdot 15\%H_2O$ colloid solution and ultra-pure water were stirred at room temperature at 1:3 volume ratio for 2 hours, and the solution was spin coated on

ITO glass at 4000 rpm for 30 seconds, and annealed at 150°C for 30 minutes.

Perovskite film: MAI and PbI_2 were dissolved 1:1 in a solution of 800 μL DMF and DMSO (volume ratio 4:1) and stirred at 60 °C for 2 hours; The solution was spin coated on SnO_2 film at 3500 rpm for 40 seconds, then 300 μL chlorobenzene solution was added at positive 10 seconds and annealed at 130 °C for 10 minutes.

Spiro-OMeTAD film: 73.2 mg Spiro-OMeTAD was dissolved in 1000 μL CB, 28.8 μL t-BP and 17.6 μL LiTFSI solution (520mg·L^{-1} in acetonitrile) and stirred at room temperature for 1 hour, then spin coated on perovskite at 3000 rpm for 30 s. The device is oxidized for 20 hours.

Au electrode: 60nm was deposited under high vacuum (< 5×10^{-4} Pa).

Carbon electrode: The carbon paste is brushed on the upper layer of perovskite at 120 °C in the absence of gold electrodes and hole transport layers.

(2) p-i-n device

NiO_x film: 290.7 mg of $Ni(NO_3)_2\cdot6H_2O$ was dissolved in 1000 μL ethylene glycol and 67 μL ethylenediamine, and stirred at 60°C for 1.5 hours. The solution was spun on ITO glass in two steps at 600 rpm, 8s and 2500 rpm, 80s respectively. And gradient annealing at 300°C for 60 minutes.

Perovskite film: The remaining conditions are the same as those for spin coating of the upright device except that the annealing temperature is 70°C.

C60 film: 25 nm was deposited under high vacuum (< 5×10^{-4} Pa);

ALD Al_2O_3 film: Except that the reaction chamber temperature is set to 100°C and the deposition thickness is 55 cycles of about 5.5 nm Al_2O_3 layer, the other conditions are the same as the ALD Al_2O_3 parameters when the instrument is installed.

BCP and Ag were deposited at 6 nm and 120 nm respectively under high vacuum (<5×10^{-4} Pa).

2. Characterization

AFM: The surface morphology of films was characterized by AFM (Park, XE-70).

Contact angle measurement: The contact angles of water on different sample

surfaces were measured using a contact angle meter (Kruss GmbH, DSA1005).

The thickness of the film is measured by a step meter (KLA Tencor, P-7) and an elliptical polarization spectrometer (Semilab, SE-2000)

UV-visible absorption: The absorption measurements were carried out with a spectrophotometer (Shimadzu, UV-1750).

PL & TRPL: PL and TRPL measurements were conducted using a PL spectrometer (Edinburgh Instruments, FLS 980) with an excitation light source at 520 nm.

J-V: Experiments to determine the *J-V* curves and steady-state device performance of the solar cells were performed in a glovebox under AM 1.5 G condition at an illumination intensity of 100 mW/cm^2 using a Keithley 2400 source meter in combination with a solar simulator (Enlitech, SS-F5-3A), which is calibrated by a standard Si solar cell (Enlitech, SRC-2020). The n-i-p devices were characterized in a forward scan mode (from −0.2 to 1.2 V at a step of 0.02 V) The p-i-n devices were characterized in a reverse scan mode (from 1.2 to −0.2 V at a step of 0.02 V).

EIS measurement: The EIS measurements were carried out using an electrochemical workstation to investigate charge transport and recombination processes in the solar cell devices. The impedance spectra were recorded over a frequency range of 10–10^5 Hz with an AC perturbation amplitude of 20 mV. Measurements were performed under a nitrogen atmosphere to minimize environmental effects. To ensure that conclusions drawn from impedance data are valid, we also added cross-sectional SEM images of the absorbing perovskite layers (**Figure S6**), confirming that the perovskite thickness variation is within ±20 nm, and therefore does not account for the observed resistance differences.

3. Supplementary tables and figures.

Table S1. Photovoltaic parameters of the **Au** electrode devices with ALD-Al_2O_3 layer of different thickness.

		V_{oc} (V)	J_{sc} (mA cm^{-2})	*FF* (%)	PCE (%)	HI
w/o ALD-Al_2O_3	**Forward**	**1.06**	**22.48**	**58.98**	**14.10**	**0.24**
	Reverse	**1.09**	**22.33**	**75.40**	**18.45**	
5 cycles	Forward	1.04	23.68	58.01	14.36	0.24
	Reverse	1.08	23.60	74.26	18.94	
10 cycles	Forward	1.07	23.32	61.32	15.40	0.21
	Reverse	1.10	23.24	75.68	19.39	
15 cycles	Forward	1.10	22.64	68.41	17.02	0.13
	Reverse	1.11	22.56	77.69	19.51	
20 cycles	**Forward**	**1.08**	**23.43**	**65.08**	**16.48**	**0.18**
	Reverse	**1.11**	**23.44**	**77.54**	**20.20**	
25 cycles	**Forward**	**1.08**	**23.20**	**69.88**	**17.59**	**0.11**
	Reverse	**1.10**	**23.24**	**77.43**	**19.85**	
30 cycles	Forward	1.09	22.16	55.43	12.95	0.20
	Reverse	1.09	21.99	69.30	16.20	

Table S2. Photovoltaic parameters of the **carbon** electrode devices with ALD-Al_2O_3 layer of different thickness.

		V_{oc} (V)	*FF* (%)	J_{sc} (mA`cm^{-2})	Efficiency (%)
w/o ALD-Al_2O_3	Forward	0.85	46.56	19.02	7.53
	Reverse	0.91	56.13	19.29	9.81
5 cycles	Forward	0.83	43.29	21.09	7.58
	Reverse	0.89	53.84	21.26	10.19
10 cycles	Forward	0.86	43.90	20.43	7.72
	Reverse	0.90	55.47	20.70	10.31
20 cycles	**Forward**	**0.99**	**46.79**	**21.51**	**10.00**
	Reverse	**1.03**	**60.26**	**21.34**	**13.24**
30 cycles	Forward	1.00	48.35	20.40	9.85
	Reverse	1.01	54.00	20.74	11.32
40 cycles	Forward	1.00	29.92	20.17	6.02
	Reverse	1.02	41.09	19.94	8.40

Table S3. Photovoltaic parameters of the p-i-n devices with ALD-Al_2O_3 layer of different thickness.

		V_{OC} (V)	FF (%)	J_{SC} (mA`cm^{-2})	Efficiency (%)
control	Forward	1.09	70.70	19.56	15.10
	Reverse	1.08	65.04	19.58	13.72
BCP	Forward	1.07	75.06	21.81	17.50
	Reverse	1.05	67.73	21.71	15.38
ALD Al_2O_3	Forward	1.07	80.18	20.87	17.86
50 cycles	Reverse	1.03	60.98	20.40	12.78
ALD Al_2O_3	**Forward**	**1.09**	**78.31**	**22.14**	**18.91**
55 cycles	**Reverse**	**1.06**	**67.55**	**21.76**	**15.67**
ALD Al_2O_3	Forward	1.07	76.33	21.83	17.81
60 cycles	Reverse	1.04	61.31	21.43	13.69
ALD Al_2O_3	Forward	1.06	72.64	19.88	15.29
65 cycles	Reverse	1.04	58.71	19.28	11.74
ALD Al_2O_3	Forward	1.09	70.70	19.56	15.10
70 cycles	Reverse	1.08	65.04	19.58	13.72

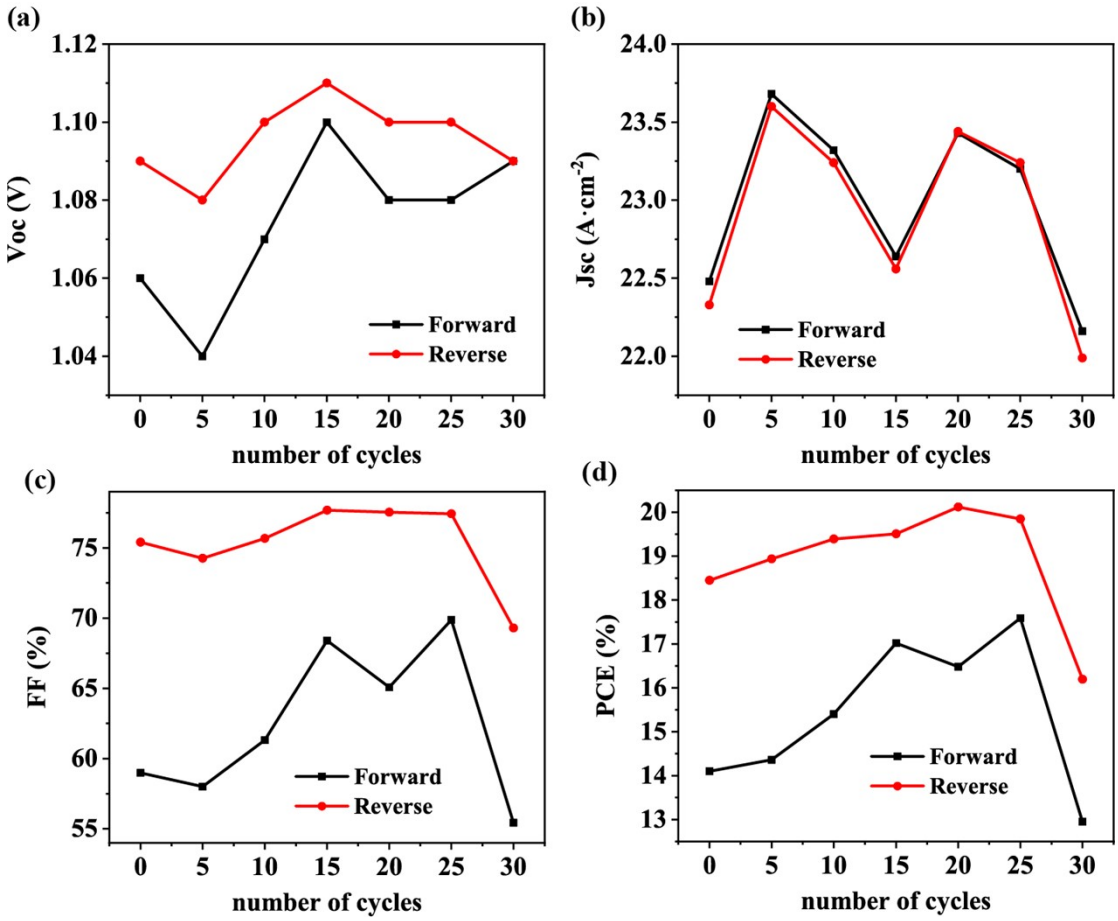

Figure S1. Plot of photovoltaic parameters as a function of ALD cycle number for both forward and reverse scans.

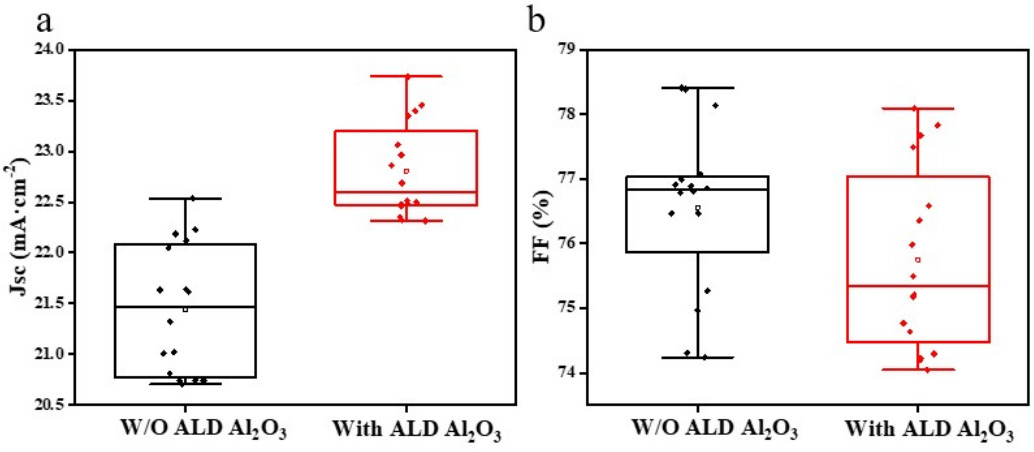

Figure S2. Distribution plots of the (a) J_{sc} and (b) FF of the Au electrode devices with (red) or without (black) 20 cycles ALD-Al_2O_3 interface layer, collected from 18 devices.

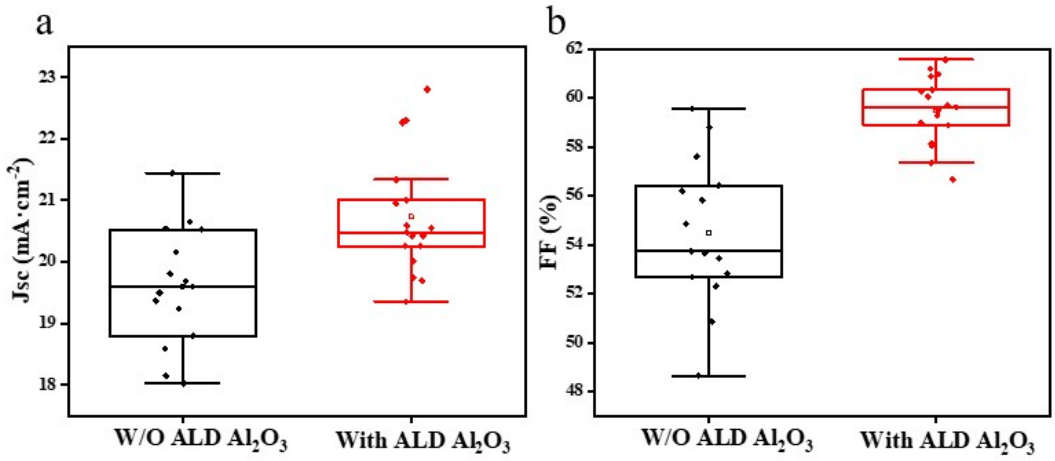

Figure S3. Plot of the (a) J_{sc} and (b) FF of the carbon electrode devices with (red) or without (black) 20 cycles ALD-Al_2O_3 interface layer, collected from 18 devices.

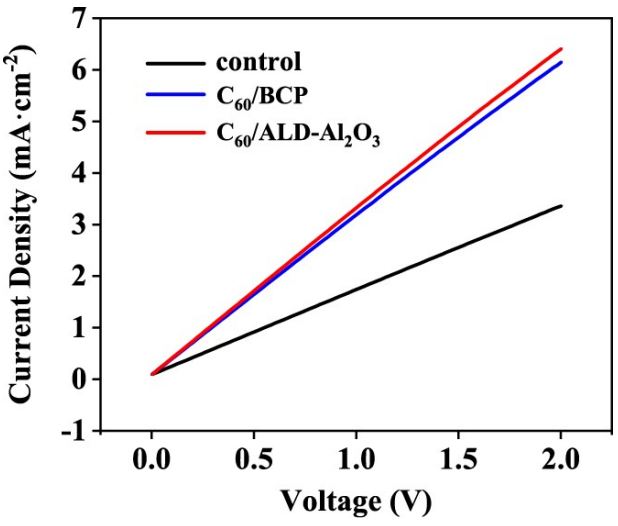

Figure S4. *J–V* curves of pure C60 (control), C60/BCP, and C60/ALD-Al_2O_3 structured devices for the conductivity comparison.

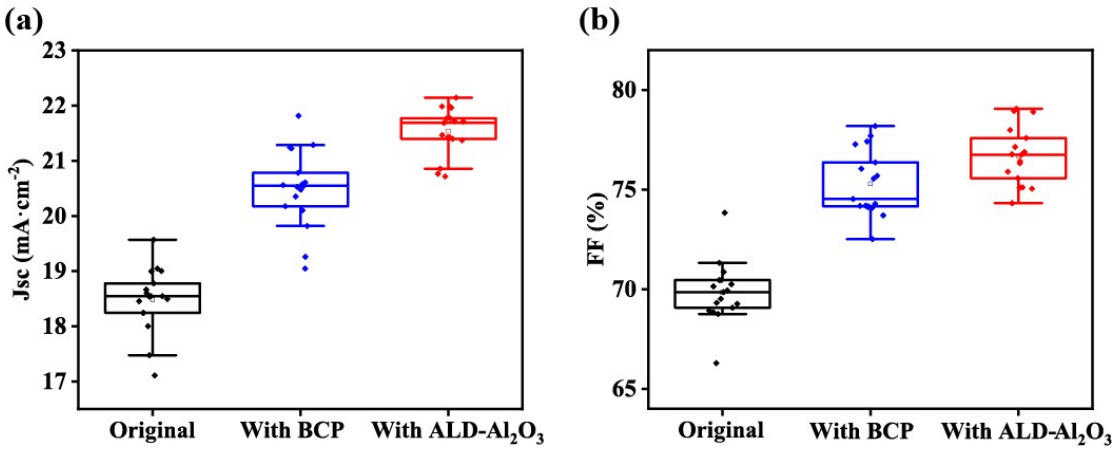

Figure S5. Data points distribution diagrams of the (a) J_{sc} and (b) *FF* of the p-i-n devices with different interface buffer layer, collected from 18 devices (red for 55 cycles ALD-Al_2O_3 devices, blue for BCP devices and black for control devices).

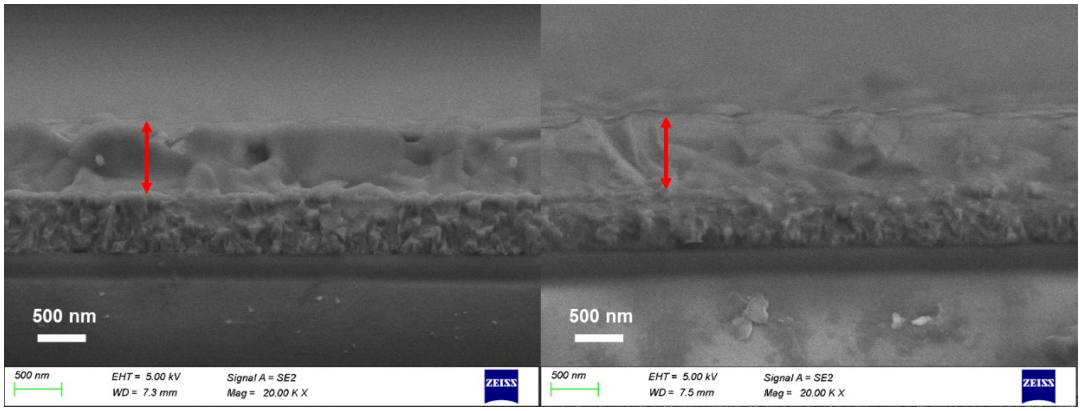

Figure S6. Cross-sectional SEM images of the perovskite absorbing layers on SnO_2/ITO substrates with and without ALD-Al_2O_3 buffer.